Dental Biomaterials: From Fundamental Principles to Clinical Applications

Dental Biomaterials: From Fundamental Principles to Clinical Applications

Editor

Mary Anne Melo

MDPI • Basel • Beijing • Wuhan • Barcelona • Belgrade • Manchester • Tokyo • Cluj • Tianjin

Editor
Mary Anne Melo
General Dentistry
University of Maryland
School of Dentistry
Baltimore
United States

Editorial Office
MDPI
St. Alban-Anlage 66
4052 Basel, Switzerland

This is a reprint of articles from the Special Issue published online in the open access journal *International Journal of Molecular Sciences* (ISSN 1422-0067) (available at: www.mdpi.com/journal/ijms/special_issues/noveldental_materials).

For citation purposes, cite each article independently as indicated on the article page online and as indicated below:

Lastname, A.A.; Lastname, B.B. Article Title. *Journal Name* **Year**, *Volume Number*, Page Range.

ISBN 978-3-0365-7725-8 (Hbk)
ISBN 978-3-0365-7724-1 (PDF)
doi.org/10.3390/books978-3-0365-7724-1

Cover image courtesy of Mary Anne Melo

Contents

About the Editor

Mary Anne Melo

Mary Anne Melo (DDS, MSc, Ph.D., Fellow ADM) is a Clinical Professor at the University of Maryland School of Dentistry and currently serves as Chair of the Department of General Dentistry. Dr. Melo applies her experience as a dentist and dental materials researcher to advance the development of smart and bioactive restorative materials. Her clinical areas of interest focus on minimally invasive dentistry, the management of patients with high-risk caries, and esthetic dentistry. Her research has focused chiefly on anticaries approaches for caries-inhibiting, antibacterial, or remineralization functionalities. Her research group has pioneered the investigation of antibacterial and remineralizing dental adhesives and resin composites. Dr. Melo is a current member of the Academy of Operative Dentistry, the International Association for Dental Research, the American Academy of Cariology, and the American Academy of Cosmetic Dentistry. Dr. Melo is a co-inventor on two patents, has edited three books, and has published more than 200 papers in the area of dental materials. Several grants support her research. She lectures nationally and internationally on diverse topics in restorative dentistry.

Preface to ”Dental Biomaterials: From Fundamental Principles to Clinical Applications”

Despite significant advancements in dental biomaterials, there are still unmet needs in the field of dentistry. The oral environment is highly complex, requiring dental materials to perform effectively under diverse physiological conditions. Therefore, it is crucial to establish methods for evaluating the performance of these materials in physiologically intricate environments that simulate real-world intraoral conditions.

Furthermore, the evolution of preventive and therapeutic strategies aimed at enhancing oral health outcomes is an ongoing process. Innovative approaches are being developed to prevent and treat common oral diseases, such as dental caries, periodontitis, and oral cancer. Researchers are also exploring the potential applications of biomaterials in regenerative dentistry, including stimulating bone growth and repairing damaged oral tissues.

Collectively, continuous research and development in dental materials and biomaterials offer promising prospects for enhancing oral health outcomes. However, it is essential to sustain ongoing research efforts to fully capitalize on their potential and effectively address the unmet needs within the dental field.

In the Special Issue titled “Dental Biomaterials: From Fundamental Principles to Clinical Applications,“ a range of valuable findings have emerged from diverse sources, including in vitro experiments and clinical trials. These insights have deepened our understanding of the biology of oral diseases, leading to the development of innovative treatment approaches such as targeted drug delivery systems and gene therapy. Clinical trials have also provided evidence regarding the efficacy and safety of these novel treatment options.

Overall, these technological and treatment advancements offer hope for improved management of oral diseases. However, it is crucial to emphasize the necessity for ongoing research and development to fully harness the potential of these innovations and make substantial progress in enhancing oral health outcomes.

Mary Anne Melo
Editor

International Journal of
Molecular Sciences

MDPI

Article

Dental Material Selection for the Additive Manufacturing of Removable Complete Dentures (RCD)

Dmitry I. Grachev [1], Evgeny A. Chizhmakov [2], Dmitry Yu. Stepanov [3], Dmitry G. Buslovich [4], Ibragim V. Khulaev [5], Aslan V. Deshev [6], Levon G. Kirakosyan [1], Anatoly S. Arutyunov [2], Svetlana Yu. Kardanova [5], Konstantin S. Panin [7] and Sergey V. Panin [3,*]

1 Digital Dentistry Department, A.I. Yevdokimov Moscow State University of Medicine and Dentistry, 127473 Moscow, Russia
2 Prosthodontics Technology Department, A.I. Yevdokimov Moscow State University of Medicine and Dentistry, 127473 Moscow, Russia
3 Laboratory of Mechanics of Polymer Composite Materials, Institute of Strength Physics and Materials Science of Siberian Branch of Russian Academy of Sciences, 634055 Tomsk, Russia
4 Laboratory of Nanobioengineering, Institute of Strength Physics and Materials Science of Siberian Branch of Russian Academy of Sciences, 634055 Tomsk, Russia
5 Institute of Dentistry and Maxillofacial Surgery, Kabardino-Balkarian State University Named after H.M. Berbekov, 360004 Nalchik, Russia
6 Laboratory of Digital Dentistry, Kabardino-Balkarian State University Named after H.M. Berbekov, 360004 Nalchik, Russia
7 Department of Chemical Physics, Institute for Laser and Plasma Technologies, National Research Nuclear University MEPhI, 115409 Moscow, Russia
* Correspondence: svp@ispms.ru

Abstract: This research addresses the development of a formalized approach to dental material selection (DMS) in manufacturing removable complete dentures (RDC). Three types of commercially available polymethyl methacrylate (PMMA) grades, processed by an identical Digital Light Processing (DLP) 3D printer, were compared. In this way, a combination of mechanical, tribological, technological, microbiological, and economic factors was assessed. The material indices were calculated to compare dental materials for a set of functional parameters related to feedstock cost. However, this did not solve the problem of simultaneous consideration of all the material indices, including their significance. The developed DMS procedure employs the extended VIKOR method, based on the analysis of interval quantitative estimations, which allowed the carrying out of a fully fledged analysis of alternatives. The proposed approach has the potential to enhance the efficiency of prosthetic treatment by optimizing the DMS procedure, taking into consideration the prosthesis design and its production route.

Keywords: PMMA; additive manufacturing (AM); material selection; analytic hierarchy process (AHP); VIKOR; multicriteria decision-making (MCDM); material index; ranking

Citation: Grachev, D.I.; Chizhmakov, E.A.; Stepanov, D.Y.; Buslovich, D.G.; Khulaev, I.V.; Deshev, A.V.; Kirakosyan, L.G.; Arutyunov, A.S.; Kardanova, S.Y.; Panin, K.S.; et al. Dental Material Selection for the Additive Manufacturing of Removable Complete Dentures (RCD). *Int. J. Mol. Sci.* **2023**, *24*, 6432. https://doi.org/10.3390/ijms24076432

Academic Editor: Lia Rimondini

Received: 28 February 2023
Revised: 20 March 2023
Accepted: 27 March 2023
Published: 29 March 2023

1. Introduction

Material selection is a relevant issue that is solved in various branches of science and technology, inter alia dental treatment (for example, manufacturing RCD). In this case, components are calculated according to the strength criterion (by the finite element method [1], as an example) and assigned margin factors. Therefore, reference data (primarily, manufacturers' data sheets) should be taken into account. Typically, the most appropriate materials have to be selected for various functional applications. For this purpose, (i) the elastic modulus is considered to ensure a required stiffness level, (ii) crack resistance is controlled by fracture toughness, and (iii) corrosion resistance can be characterized either qualitatively or quantitatively according to the parameters measured by strictly regulated industrial standards, etc. In addition to physical and mechanical characteristics, designers consider

(i) the material manufacturability (including the possibility of 3D printing, CAD milling, etc.), (ii) the variation of properties under heat treatment (for example, annealing)/post-build processing (additional polymerization, as an example), and (iii) machinability with various types of tools (grinding), etc. [2].

DMS with such a formalized approach can be solved if several required (target) characteristics are considered, among them: (a) physical and mechanical; (b) biological; (c) functional (color, polishability, roughness, etc.); (d) technological (processing methods, machinability, warpage); (e) cost, etc. Nevertheless, medical treatment tactics for the use of (temporal) dental prosthetics are a multifactorial problem. Therefore, the mission of DMS, including prosthesis manufacturing methods, becomes more complex. In practice, it is greatly affected by the mostly subjective relationships in the group "dentist–dental technician–patient" [3].

Despite the necessity of using temporary dentures, the attitude of maxillo-facial surgeons, dentists and patients to such structures is rather dismissive. To this end, breakdowns and complications are frequent due to medical and technical errors. In practical dentistry, there is a need for enduring polymer prostheses in the treatment of complex dental pathologies that requires an accurate and long-term examination. In particular, this is relevant for diagnosing gnathic problems, especially in cases of muscular–articular dysfunction. Therefore, such therapeutic and prophylactic orthopedic constructions play an important role in first-stage rehabilitation measures. These include periods of (i) temporary filling of a defect in the dentition, (ii) programming a new occlusion, (iii) osseointegration of dental implants, etc. [4–6]. Hence, the practice of using temporary dentures remains very important.

The State of the Art in the Additive Manufacturing of RDC

RCDs for edentulous patients are typically made of PMMA [7]. However, a high concentration of free monomer (methyl methacrylate) and the possible development of allergic stomatitis is a significant drawback of this material [8].

Up-to-date CAD/CAE/CAM systems are frequently implemented into dental practice. They provide (i) great shape and dimensional accuracy, (ii) reproducibility, (iii) minimization of medical and technical routine work, (iv) cost reduction, and therefore (v) the availability of highly efficient dentures and facial epithesis [9,10]. However, additive manufacturing (AM) demands novel classes of polymers. In addition, the CAM process (as a subtractive method) possesses the following drawbacks: (i) material waste due to grinding and milling, (ii) wear of cutting tools and expensive equipment, (iii) restrictions on the sizes of the blanks (in the form of blocks) which does not allow the fabrication, for example, of volumetric jaw prostheses-obturators [11].

In this way, 3D printing is an actual trend in dental practice. Studies of physical–mechanical characteristics and aesthetics of such volumetric structures are highly controversial when polymeric prostheses or medical devices must be designed for long-term use (for example, in the case of parafunctional phenomena, or when an occlusion is to be reprogrammed) [12]. The quality of the AM structures depends on 3D printing parameters, building accuracy, shape, and dimensions of a virtual model, among many others [13]. Currently, a wide variety of 3D printers are available, including various physical principles of layer-by-layer deposition. To this end, prosthesis accuracy is a tangible drawback [14,15]. However, the prospects of AM in dentistry are beyond dispute [16].

Laser stereolithography apparatus (SLA) employs liquid photopolymers that are cured with a laser beam or an ultraviolet (UV) source of a certain wavelength. Product quality is affected by the dimensions of a prototype, the angle of the 3D-printed object related to the platform, the locations of supports, etc. Besides economic efficiency, such procedures are convenient for planning surgical operations with parts of a complex shape and structure [17].

The durability of (temporary) RDC depends on their design features, physical–chemical nature of the structural materials, and production routes [18]. Karaokutan et al. studied the influence of manufacturing techniques for provisional PMMA-based crowns on their

strength characteristics [19]. The authors reported that computer-controlled milling improves the strength of the temporary RDC, compared to those fabricated by a direct manufacturing method. Alt et al. presented a comparative study of the strength characteristics of temporary polymer bridges made by conventional and digital technologies and concluded that the manufacturing methods substantially affect their values [20].

Dikova showed that high dimensional accuracy and surface smoothness of fixed dentures can be achieved when the vertical axis of teeth coincides with the *Z* axis of a platform [21]. At the same time, the number of supports should be increased (at least four per tooth) to reduce warpage in 3D printing and post-build polymerization. Thus, to ensure a high-quality product in designing and planning the process, it is important to consider the following: (i) printer characteristics, (ii) model placement, (iii) number of supports, and (iv) dimensional variation during and after polymerization.

Li suggested that the high-quality manufacture of temporary polymer prostheses be provided by the SLA method based on temperature-controlled layer-by-layer deposition in 3D printing (TCMIP-SL) [22]. The TCMIP-SL process contributes to the deposition of high-viscosity polymers with excellent accuracy at high speeds.

Based on the above, it can be stated that searching for dental AM materials with improved quality has moved into the phase of developing optimal dental technologies that use industrial polymers and help to minimize fabrication process disruptions that deteriorate a product's characteristics.

This paper addresses the development of a formalized approach for DMS and the additive manufacturing of RCD. This issue was solved using a decision-making methodology. Rational ranking was illustrated on examples of three types of commercially available PMMA grades processed by the identical DLP method. The paper is structured as follows. Section 2 describes the 3D printing method and techniques for evaluating the key properties of the AM blanks. Section 3 contains the measurement results for various characteristics of dental materials; the calculation of the material indices is also provided. Section 4 proposes the approach to multicriteria optimization in DMS and examples of their ranking as well. Section 5 discusses the obtained data. The authors proposed, based on examples of certain industrially produced brands, an approach to (or the tool for) brand ranking; the variability of the results was emphasized. Recommendations to use one or another brand of dental materials remain for individual consideration.

2. Materials and Methods

2.1. Three-dimensional Printing (Materials and Equipment)

The test samples were fabricated in two stages: modeling and 3D printing. Virtual master models were created using the ExoCad Gateway 3.0 software (Align Technology, San Jose, CA, USA). The final files of the completed sample models (in the "*.STL" format) were imported into the (slicer) software package for the 3D printing preparation. Then, (i) the models were positioned relative to the plane of the 3D printer platform, (ii) the supports were placed, (iii) the models were divided into layers, and (iv) the 3D printing parameters were adjusted in line with recommendations of the feedstock manufacturers (Table 1).

Table 1. The data on the 3D printing materials and methods.

Material	FreePrint, Temp 385, A2	Nolatech	Dental Sand, A1–A2
Designation in the text	FP	NT	DS
Manufacturer	DETAX GmbH & Co. KG (Germany)	Nolatech (Russia)	Harz Labs (Russia)
3D printer		NextDent 5100; (3DSystem, USA)	
Software for constructing digital models		3DSprint (3DSystem, USA)	
3D printing technology		Digital Light Processing (DLP)	
Thickness of a single printed layer		50 μm	
Post-build processing	Anycubic Wash & Cure 2.0 (Cleaning with 70% isopropyl alcohol for 3 min, UV curing)		

2.2. Property Evaluation Methods

Comparative studies of the mechanical, tribological, technological, biological, and economic characteristics of dental materials were performed. Mechanical tests were carried out for tension, compression, and three-point bending. In this paper, only the three-point bending data are reported, since they are more informative for the dental materials [23]. The key parameters to be evaluated are flexural strength, flexural modulus, and flexural strain.

2.2.1. Three-Point Bending Tests

The samples took the form of rectangular plates with dimensions of 25 × 2 × 2 mm following the Russian State Standard GOST 31574-2012. An "Instron 5982" electromechanical testing machine (Illinois Tool Works Inc., Glenview, IL, USA) was used with a crosshead speed of 0.75 mm/min. The force gauge had an upper measurement limit of ± 5000 N (series 2580–108). The span was 20 mm. Before testing, the samples were conditioned in distilled water at a temperature of 37 ± 1 °C for 24 h. The tests were carried out until the sample failure.

2.2.2. Impact Strength Tests

The a_n Charpy impact strength of specimens without a notch was measured with a "KM-5" pendulum impact tester ("ZIP" LLC, Ivanovo, Russia). Their sizes were 80 × 10 × 4 mm according to the Russian State Standard GOST 4647-2015. There were four specimens of each material. After the tests, the average a_n values were calculated.

2.2.3. Biological Tests

For biological tests, the samples were in the form of disks 5 mm in diameter and 1 mm thick. The attachment points for supports were finished with the polishes of various abrasiveness in the following sequence: 9400.204.030, 9401.204.030, 9402.204.030 (Komet, Gebr. Brasseler GmbH & Co. KG, Germany). The time lag from sample fabrication to the biological tests did not exceed 72 h. Immediately before the start of the in vitro experiment, the samples were cleaned in an ultrasonic bath for 15 min, after they were treated with 70% ethanol.

To carry out the process of the primary adhesion of microorganisms, the samples were placed in test tubes with a suspension of the test strains of the corresponding species at a standard concentration. We used the optical turbidity standard of 0.5 U McFarland, which corresponded to 10^9 colony-forming units (CFU)/mL for bacterial cultures and 10^8 CFU/mL for yeast ones. After quantitative inoculation, bacteria were cultivated under anaerobic conditions at a temperature of 37 °C for 7 days, and fungi—at room temperature (25 °C) for 2 days. Adhesion indices were determined as a ratio of the decimal logarithm of the number of CFU obtained after sonication of the test samples to the decimal logarithm of the CFU of the initial microbial suspension. The authors described the experimental technique in detail in their previous paper [7].

2.2.4. Tribological Tests

In the point tribological contact according to the "ball-on-disk" scheme, the dry sliding friction tests were carried out at a load (P) of 5 N and a sliding speed (V) of 0.3 m/s. A "CH 2000" tribometer (CSEM, Neuchâtel, Switzerland) was used following ASTM G99. The tribological tests were conducted using a ceramic counterpart (a ball made of the ZrO_2) with a diameter of 6 mm and the R_a surface roughness of 0.02 μm. The latter was assessed with the "New View 6200" optical interferential profilometer (Zygo Corporation, Middlefield, CT, USA). The testing distance was 1 km and the tribological track radius was 10 mm.

In the linear tribological contact according to the "block-on-ring" scheme, dry sliding friction tests were performed using a "2070 SMT-1" friction testing machine (Tochpribor Production Association, Ivanovo, Russia). A load (P) was 60 N, while a sliding speed (V) was 0.3 m/s. A ceramic counterpart was made of an Al_2O_3 ring with a diameter of

35 mm and a width of 11 mm. The R_a surface roughness was 0.20 µm. The counterpart temperatures were assessed with the "CEM DT-820" non-contact infrared (IR) thermometer (Shenzhen Everbest Machinery Industry Co., Ltd., Shenzhen, China).

WR levels were determined by measuring the width and depth of wear tracks according to a stylus profilometry (KLA-Tencor, Milpitas, CA, USA), followed by multiplication by their length. They were calculated taking into account load and distance values:

$$\text{Wear rate } = \frac{\text{volume loss } (\text{mm}^3)}{\text{load } (\text{N}) \times \text{sliding distance } (\text{m})} \quad (1)$$

In the flat tribological contact, abrasion wear tests were conducted. The "MI-2" abrasion testing machine (Metroteks LLC, Moscow, Russia) was used to determine the weight loss values at abrasion by fixed particles, according to the "polymer pin-on-abrasive disk" scheme (Figure 1b), regulated by the Russian State Standard GOST 426-77. The dimensions of the samples were 8 × 10 × 8 mm. The average grain size of an abrasive paper (P1000) was ~17 µm. The angular sliding velocity was 40 rpm, and the load was 10 N. The test scheme is shown in Figure 1a.

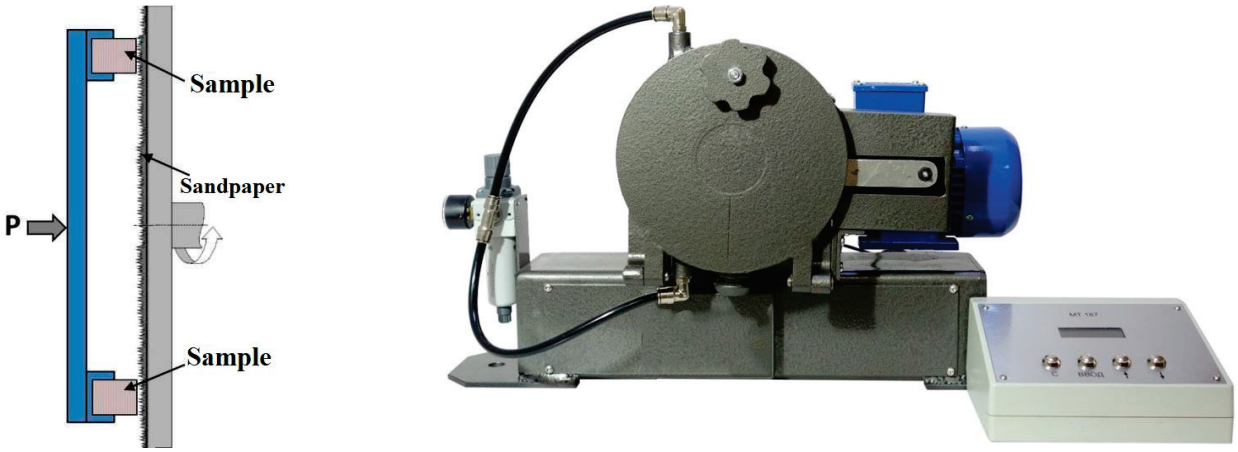

(**a**) (**b**)

Figure 1. A scheme of the abrasive wear tests (**a**) and the "MI-2" abrasion testing machine (**b**).

Weight loss was determined every 5 min during the total test duration of 20 min. The samples were weighed using the "Sartogosm LV 120-A" (Sartogosm LLC, Saint Petersburg, Russia) with an accuracy of 0.1 mg.

2.2.5. Polishability (via Roughness)

The protocol for grinding and polishing in the sample preparation procedure is presented below.

1. Surface treatment with a carbide cutter for polymers until the required configuration or shape.
2. Surface treatment with a carbide cutter for polymers to remove surface irregularities.
3. Sanding with 180–220 grit sandpaper for extra fine finishing.
4. Finishing with a felt and a moistened polishing powder.
5. Brushing with a grinder using a coarse bristle and a moistened polishing powder for a smooth surface.
6. Processing with a grinder using a thread brush and a fine-grained polishing paste to a mirror finish.

The R_a surface roughness was assessed with the "New View 6200" optical interferential profilometer (Zygo Corporation, Middlefield, CT, USA).

3. Results

3.1. Mechanical Properties

The mechanical properties of the SLA 3D-printed PMMA samples, registered in the three-point bending tests, are presented in Table 2. For the Dental Sand (DS), the flexural strength and strain values exceed by ~10 % and two times the corresponding characteristics for Free Point (FP), as well as by 2.5 and 3.6 times for Nolatech (NT), respectively. For all the studied PMMA grades, the flexural modulus values were at the same level of about 2.7 ± 0.1 GPa.

Table 2. The mechanical properties of the 3D printed PMMA of the studied grades.

No.	Material	Flexural Modulus, GPa	Flexural Strength, MPa	Flexural Strain, %
1	FP	2.7 ± 0.6	90.7 ± 5.9	2.7 ± 0.6
2	NT	2.8 ± 0.1	41.7 ± 4.5	1.5 ± 0.1
3	DS	2.6 ± 0.3	104.2 ± 2.7	5.4 ± 1.2

Since PMMA RCD could experience impact in use (for example, being accidentally dropped on ceramic tiles), their impact strength could be an important performance characteristic. The conducted Charpy impact tests showed that a_n values were 0 J/cm^2 at the minimum applied impact energies regardless of the PMMA grade. Thus, it was impossible to differentiate the materials by this parameter. Please note that an increase in impact strength could be achieved by loading PMMA with fibers or nanoparticles in various concentrations, but this would change the manufacturability of the materials, including the possibility of their AM processing [24–26].

3.2. Biological Properties

The adhesion indices (AIs) of the normal, periodontopathogenic, and fungal microbiota to the studied materials are presented in Table 3. In the normal microbiota case, no differences were found between the FP (0.55 ± 0.06) and the NT (0.56 ± 0.06). For the DS, a value of 0.43 ± 0.06 was noticeably lower than those for the other two materials. For the periodontopathogenic microbiota, an AI value of 0.42 ± 0.05 for the NT was noticeably higher than those for the DS and the FP, for which no significant differences were found (AI = 0.34 ± 0.05). In the fungal microbiota case, some variations were observed for all the materials. The maximum level was typical for the NT (AI = 0.49 ± 0.05), and the minimum was detected for the DS (AI = 0.34 ± 0.05).

Table 3. The adhesion indices of the normal, periodontopathogenic, and fungal microbiota to the materials under study.

No.	Material	Normal	Periodontopathogenic	Fungal
1	FP	0.55 ± 0.06	0.34 ± 0.05	0.43 ± 0.02
2	NT	0.56 ± 0.06	0.42 ± 0.05	0.49 ± 0.05
3	DS	0.43 ± 0.06	0.34 ± 0.05	0.34 ± 0.05

3.3. Tribological Properties

3.3.1. The Point Tribological Contact

The point tribological contact involved a local impact of the ceramic ball on the polymer sample (in the form of a disk) under dry sliding friction conditions. Table 4 presents the values of the tribological properties of the materials under study. The FP and DS had the lowest coefficient of friction (CoF) values (0.276 and 0.271, respectively), while it was higher by 10 % (0.303) for the NT (Figure S1). The wear rate (WR) levels were also evaluated. For the FP, it was half that for the NT and DS. Roughness on the wear friction track surfaces was approximately at the same level of 0.19 μm regardless of the PMMA grade.

Table 4. The tribological properties of the PMMA dental materials in the point tribological contact.

No.	Material	Coefficient of Friction, CoF	Wear Rate, WR, $mm^3/N \cdot m$, 10^{-5}	Wear Track Roughness, Ra, μm
1	FP	0.276 ± 0.019	13.52 ± 1.01	0.191 ± 0.030
2	NT	0.303 ± 0.025	26.97 ± 0.91	0.204 ± 0.026
3	DS	0.271 ± 0.022	28.29 ± 0.98	0.179 ± 0.015

3.3.2. The Linear Tribological Contact

In the linear tribological contact, the ring-shaped ceramic counterpart slid relative to the stationary polymer samples, along the "non-renewable" surface of the wear tracks. Therefore, the specific pressure was noticeably lower compared to that in the point tribological contact. As a result, the average CoF values were lower by ~3 times for all the studied materials (0.131, 0.096, and 0.122, respectively, according to Table 5). The NT had the lowest WR level of 0.078×10^{-6} $mm^3/N \cdot m$, which was 2.3 times lower compared to that for the DS and 1.5 times than that for the FP (Figure S2). In contrast to the point tribological contact, the WR values were an order of magnitude lower (10^{-5} and 10^{-6}, respectively).

Table 5. The tribological properties of the PMMA dental materials in the linear tribological contact.

No.	Material	Coefficient of Friction CoF	Wear Rate, WR, $mm^3/N \cdot m$, 10^{-6}	Temperature, °C
1	FP	0.131 ± 0.018	0.120 ± 0.007	31.43 ± 1.50
2	NT	0.096 ± 0.016	0.078 ± 0.013	33.31 ± 0.21
3	DS	0.122 ± 0.018	0.176 ± 0.017	36.59 ± 0.99

3.3.3. The Flat Tribological Contact, Abrasive Wear

Since PMMA prostheses could be worn out by hard particles, abrasive wear tests were conducted according to the "polymer pin-on-abrasive disk" scheme. It was shown that the least wear (weight loss) was observed for the FP (0.12 mg) after 20 min of testing (with abrasive particles fixed on the non-renewable surface of the abrasive counterpart), which was 1.6 times less compared to that for the DS (0.19 mg) and 2.0 times less compared to the NT (0.25 mg) (Figure S3).

Table 6 summarizes the data on the WR values in the point, linear, and flat tribological contacts used to calculate the material indices.

Table 6. The summarized data on the WR values in the point, linear, and flat tribological contacts.

No.	Material	WR, Point Contact, $mm^3/N \cdot m$, 10^{-5}	WR, Linear Contact, $mm^3/N \cdot m$, 10^{-6}	(Abrasive) Weight Loss, Flat Contact, Δm, gr
1	FP	13.52 ± 1.01	0.120 ± 0.007	0.121 ± 0.01
2	NT	26.97 ± 0.91	0.078 ± 0.013	0.255 ± 0.01
3	DS	28.29 ± 0.98	0.176 ± 0.017	0.193 ± 0.01

3.4. Technological Properties

A significant number of the parameters could be qualified as "technological properties". Since the study deals with DMS concept development, to simplify the process, the authors limited themselves to only three ones (Table 7).

Table 7. The technological properties of 3D-printed PMMA materials.

No.	Material	Average Duration of 3D Printing and Post-Polymerization Processing, min	Roughness after Standard Polishing, Ra, μm	Warpage after 3D Printing (Quality)
1	FP	33 + 30 = 63	0.048 ± 0.005	–(0)
2	NT	33 + 50 = 88	0.049 ± 0.007	+(1)
3	DS	80 + 30 = 110	0.051 ± 0.003	–(0)

The first parameter was determined by the average duration of 3D printing and post-build polymerization processing. Its minimum value was typical for the FP (t = 63 min), while the maximum for the DS was (t = 110 min).

The second parameter was polishability, which was related to the ability of the 3D-printed PMMA products to achieve the required degree of gloss, determined by the surface roughness. In general, all the studied materials could be considered to be similar in terms of their values (R_a ~ 0.048–0.051 μm).

The third parameter was shape distortion (warpage) [27]. This was assessed qualitatively, being associated with the ability of a 3D-printed product to retain its shape after cooling. From this point of view, the NT was the only material characterized by warpage after 3D printing and post-build polymerization processing. To use these data as a quantitative criterion, this parameter was assigned at a level of 0 in the absence of the shape distortion, and otherwise it was 1.

3.5. Economic Indicator (Cost)

The financial aspects of manufacturing PMMA prostheses via 3D printing could also be assessed by numerous criteria, including costs of logistics, purchasing licenses, deployment of a particular type of 3D printer and its maintenance, and many others. Nevertheless, the authors implemented the only criterion, namely the feedstock cost, for simplification (since the sample fabrication was carried out with the same 3D printer). Quantitative data are given in Table 8 for all the materials under study.

Table 8. The price for the dental material feedstocks (February 2023).

No.	Material	Price for 1 kg, US Dollar
1	FP	USD 381
2	NT	USD 203
3	DS	USD 404

3.6. Ranking Materials by Indices

The following parameters were introduced in the study according to the concept of the material indices proposed by Ashby [2] (as a ratio of the data presented in Tables 2–7 to the feedstock costs in Table 8). The charts of the material indices are shown in Figure 2. Their values were obtained by dividing the factors by the feedstock costs and multiplying by 100, they are:

- M1 is the ratio of the mechanical properties to the feedstock cost (namely flexural modulus, flexural strength, and flexural strain);
- M2 is the ratio of the biological properties to the feedstock cost (all three types of the studied microbiota were considered);
- M3 is the ratio of the tribological properties to the feedstock cost (a wear resistance for all three schemes of the tribological tests);
- M4 is the ratio of the technological properties to the feedstock cost (the average duration of 3D printing and post-build polymerization processing, roughness after standard polishing, and warpage after 3D printing).

To this end, the use of the concept of material indices (Tables S1–S4) offered a clear tool for quantitative comparison of the dental materials in the case under study. Moreover, it was possible to choose (from the point of view of a user or an expert) a more or less significant one. However, the significance factor was very subjective, so the analysis had to be carried out either by considering the data in a multilevel space or using multicriteria optimization approaches [28].

In the first case, an efficient method could be implemented to reduce the dimension of the analyzed data space, e.g., down to two [29–32]. The solution using the second approach is introduced in the next section.

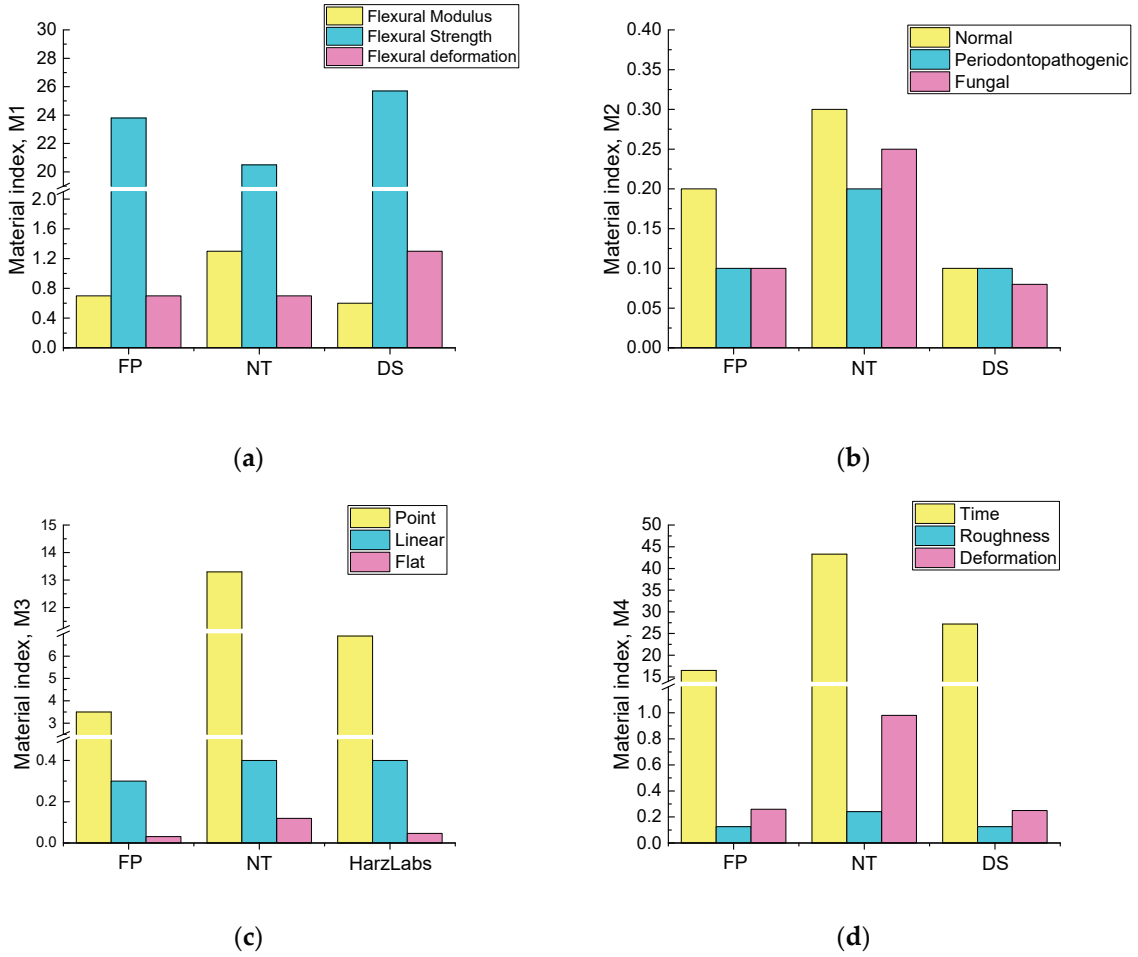

Figure 2. The material indices of the studied dental materials: M1 is the ratio of the mechanical properties to the feedstock cost (**a**), M2 is the ratio of the biological properties to the feedstock cost (**b**), M3 is the ratio of the tribological properties to the feedstock cost (**c**), M4 is the ratio of the technological properties to the feedstock cost (**d**).

4. Data Interpretation—The Combined AHP–Extended VIKOR Methods

In this section, some methods for DMS were compared, taking into account their production routes, which provided a trade-off between requirements for a set of mechanical, tribological, technological, biological, and economic criteria. The authors used informal subjective assessments of experts in the field of dental prosthetics, 3D printing, and the manufacture of CRD by subtractive and additive methods (primarily at A.I. Yevdokimov Moscow State University of Medicine and Dentistry, Russia).

4.1. The Problem Statement and Methods

Within the decision-making theory framework, the studied dental materials were qualified as decision alternatives with their designation as A_i. The factors characterizing each alternative were quantitative assessments and qualitative indicators. Based on the factors, if the criteria of (i) quality, (ii) usefulness, (iii) reliability, etc. were put forward, then the alternatives could be compared. The problem of choosing an alternative arose when there was a contradiction between the results of comparison or the absence of an alternative with the best indicators of the factors (an ideal combination of the characteristics) [33]. In this case, the problem of multicriteria optimization arose, namely the choice of a rational alternative from the available finite set, i.e., an alternative that was closest to an "ideal" option.

To date, a large number of methods for solving multicriteria optimization problems are known [34,35], i.e., Multicriteria Decision-Making (MCDM) methods. They include the

Analytic Hierarchy Process (AHP), Technique for Order of Preference by Similarity to Ideal Solution (TOPSIS), VIKOR, ÉLimination Et Choix Traduisant la REalité (ELECTRE), Preference Ranking for Organization Method for Enrichment Evaluation (PROMETHEE), etc. The key difference between these methods lies in the algorithms bringing different-scale, often qualitative, data into a single normalized space and the subsequent choice of a metric inside it. Examples of MCDM can be found both in tribology [36] and medicine [37–39], as well as in other areas [40,41]. Recently, MCDM, based on interval estimates, has been developed. For example, extended both TOPSIS and VIKOR methods were described, [42,43] while their advantages and drawbacks were reported in [44–46]. In this paper, the authors consider the possibility to implement the AHP and VIKOR ones for solving the problem of the DMS (PMMA-based) for manufacturing RCD (including the temporary ones).

4.2. Initial Data Analysis

All the data were divided into groups according to their physical meanings (Table 9). The mechanical, tribological, technological, biological, and economic groups included the experimental data in the form of interval quantitative estimations with different scales. The remaining groups were described by point quantitative values (in contrast to the interval ones). The exception was the "Warpage after 3D printing" technological factor. It was qualitative (binary) in nature and could be coded as "0" ("no warpage"), and as "1" ("might be distorted") in this case. Since the "Roughness after polishing" technological factor turned out to be identical for all the materials, it was not used in analysis and decision-making.

Table 9. The alternatives, their factors, and the criteria for the initial data analysis.

Group	Factor	Criterion	Alternative		
			A_1 FP	A_2 NT	A_3 DS
Mechanical	Flexural modulus, GPa	1	2.7 ± 0.6	2.8 ± 0.1	2.6 ± 0.3
	Flexural strength, MPa	1	90.7 ± 5.9	41.7 ± 4.5	104.2 ± 2.7
	Flexural strain, %	1	2.7 ± 0.6	1.5 ± 0.1	5.4 ± 1.2
Tribological	Wear rate, point contact, WR, $mm^3/N{\cdot}m$, 10^{-5}	–1	13.52 ± 1.01	26.97 ± 0.91	28.29 ± 0.98
	Wear rate, linear contact, WR, $mm^3/N{\cdot}m$, 10^{-6}	–1	0.120 ± 0.007	0.078 ± 0.013	0.176 ± 0.017
	(Abrasive) weight loss, flat contact, Dm, gr	–1	0.121 ± 0.01	0.255 ± 0.01	0.193 ± 0.01
Technological	Average duration of 3D printing and post-build polymerization processing, min.	–1	63	88	110
	Roughness after standard polishing, Ra, μm	–1	0.05 ± 0.00	0.05 ± 0.00	0.05 ± 0.00
	Warpage after 3D printing (quality)	–1	0	1	0
Biological	Normal, c.u.	–1	0.55 ± 0.06	0.56 ± 0.06	0.43 ± 0.06
	Periodontopathogenic, c.u.	–1	0.34 ± 0.05	0.42 ± 0.05	0.34 ± 0.05
	Fungal, c.u.	–1	0.43 ± 0.02	0.49 ± 0.05	0.34 ± 0.05
Economic	Price for 1 kg of feedstock, USD.	–1	USD 381	USD 203	USD 404

The material assessment criteria were selected separately for each factor and coded according to two principles: (+1) was the "utility" principle ("the more, the better") and (–1) was the "cost" one ("the less, the better").

4.3. Determination of Criteria Weights by the AHP Method

The AHP method was implemented to determine the weights (significance) of the criteria [47]. It referred to ones for supporting selection from a small number of alternatives based on pairwise comparisons. In this case, the formation of a matrix of the pairwise significance of the criteria was performed by an expert, and the calculation of the weights of the criteria was carried out by searching for the eigenvalues of this matrix. Due to the large number of the criteria and their different nature, the analysis of their pairwise significance was conducted within the groups, first, and between them, second. The following scale was used to assess the pairwise significance:

1—the criteria were the same;

3—the first criterion was slightly more important than the second one;

5—the first criterion was much more important than the second one;

7—the first criterion was undeniably more important than the second one, it was confirmed not only by experts but also in practice;

9—the first criterion was of absolutely greater importance than the second one.

Tables of the pairwise comparison within the groups were filled by experts from the respective fields. Therefore, despite such an assessment being subjective, the spread of opinions within the groups was low and not of interest to the research. The results of the pairwise comparison and the calculation of the weights are presented in Tables 10–13.

Table 10. The data on the paired comparison and the weights. Mechanical factors.

Criterion	Flexural Modulus	Flexural Strength	Flexural Strain	Weight
Flexural modulus	1.00	1.50	1.50	0.43
Flexural strength	0.67	1.00	1.00	0.29
Flexural strain	0.67	1.00	1.00	0.29

Table 11. The data on the paired comparison and the weights. Tribological factors.

Criterion	Wear Rate, Point Contact	Wear Rate, Linear Contact	(Abrasive) Weight Loss, Flat Contact	Weight
Wear rate, point contact	1	1	1	0.33
Wear rate, linear contact	1	1	1	0.33
(Abrasive) weight loss, flat contact	1	1	1	0.33

Table 12. The data on the paired comparison and the weights. Technological factors.

Criterion	Average Duration of 3D Printing and Post-Polymerization Processing	Warpage after 3D Printing (Quality)	Weight
Average duration of 3D printing and post-build polymerization processing	1	0.33	0.25
Warpage after 3D printing (quality)	3	1	0.75

(cerabone®, botiss biomaterials, Zossen, Germany) mixed with autologous bone that was harvested locally, around the surgical site. In both groups, the wound was primarily closed with a resorbable collagen membrane and connective tissue graft harvested from the palate using resorbable 6.0 monofilament sutures (SMI, St. Vith, Belgium, Surgicryl Rapid 6.0.) (Figures 4 and 5).

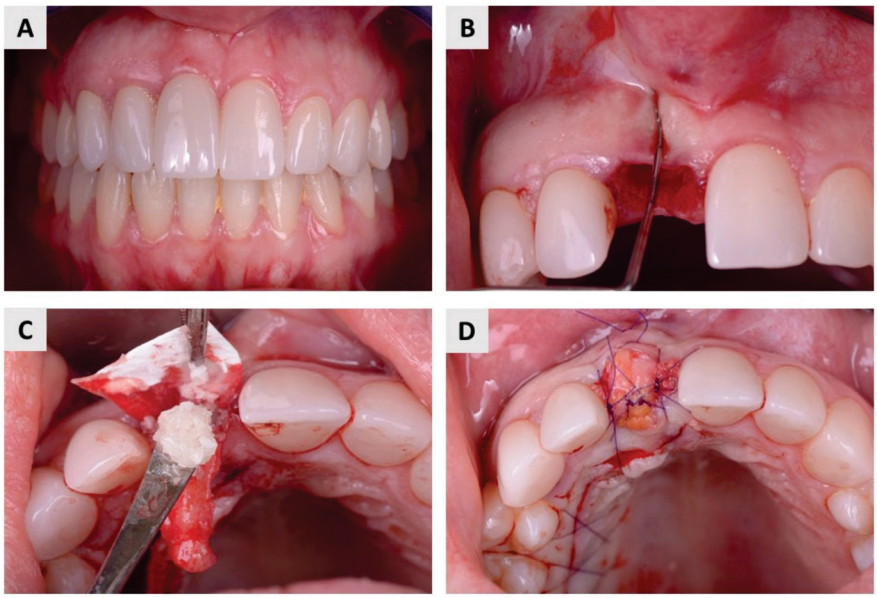

Figure 4. Surgical protocol in the test group. (**A**) The patient suffered from internal root resorption of the maxillary central incisor. (**B**) After atraumatic extraction, the integrity of the alveolar bone walls was checked with a dental probe. (**C**) An autologous dentin graft was placed in the extraction socket and covered with a resorbable membrane. (**D**) Finally, the wound was primary closed with connective tissue graft.

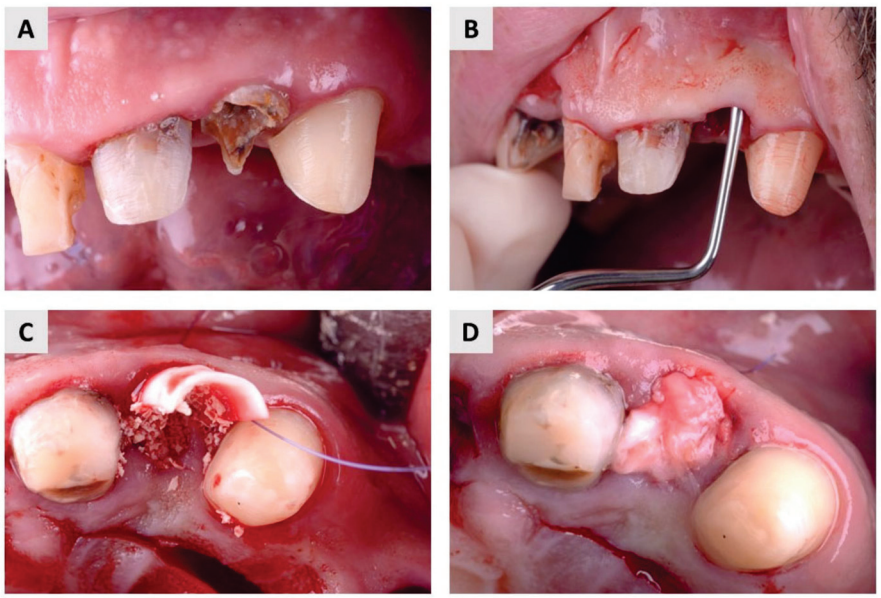

Figure 5. Surgical protocol in the control group. (**A**) A hopeless maxillary lateral incisor. (**B**) After extraction, a detailed curettage was carried out and the integrity of the alveolar bone walls was checked. (**C**) Bovine xenograft mixed with autologous bone and placed into extraction socket. A resorbable membrane was placed buccally. (**D**) Primary wound closure with connective tissue graft.

In the cases where autologous dentin graft was used, the material was prepared according to the manufacturer's recommendations [36]. The extracted teeth were thoroughly manually cleaned with a high-speed carbide bur. Before grinding, all filling materials, calculus, caries, periodontal ligament, discolored dentin and part of the enamel were removed. After drying with an air syringe, the clean teeth were ground in a sterile chamber of the Smart Dentin Grinder (SDG) (KometaBio Inc., Cresskill, NJ, USA). The SDG device was programmed to collect 300–1200 μm particles in the collection chamber. To remove all organic debris and bacteria, the particle teeth were immersed in an alcohol-based basic cleaner for 5 min in a sterile container. They were then dried with sterile gauze. The particles were then rinsed twice in sterile phosphate-buffered saline and were ready to be used as graft material.

All patients were instructed to take the prescribed antibiotics and analgesics as needed and to rinse the mouth with chlorhexidine-based fluids for one month after treatment. Follow-up examinations were performed 10, 30, and 60 days after the procedure. Four months later, patients were called again for restoration with a dental implant.

4.3. Bone Biopsy Collection

Bone biopsy was performed 4 months after bone augmentation simultaneously with implant bed preparation. Bone samples were harvested using a trephine burr with a diameter ranging from 2.3 to 2.8 mm (Helmut Zepf, Seitingen-Oberflacht, Germany) (Figure 6). The diameter of the trephine bur is smaller than that of the final burr in the implant set, which is important to avoid additional bone removal. The collected biopsies were preserved in 4% buffered paraformaldehyde and then forwarded to the laboratory for histological and immunohistochemical analysis. Finally, a dental implant (BEGO Semados RSX^{Pro}, Bego GmbH, Bremen, Germany) was placed.

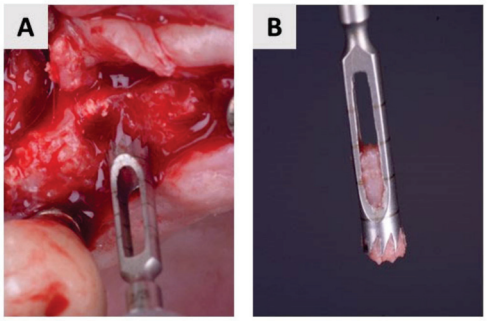

Figure 6. Biopsy collection. (**A**) Trephine bur in maxilla. (**B**) Closer view of the bone sample.

4.4. Histology and Immunohistochemistry

Fixed bone tissue samples were decalcified in Osteofast 2 solution (Biognost, Zagreb, Croatia), embedded in paraffin wax and cut into 5 μm thick tissue sections. Tissue sections were then stained with hematoxylin-eosin and examined under a light microscope with a video camera. For histomorphometric analysis, photomicrographs at 10× magnification were transferred to ImageJ v1.53 software (NIH, https://imagej.nih.gov/ij/). Histomorphometric analysis determined the percentage of newly formed bone, residual biomaterial, and soft tissue.

For immunohistochemical analysis, previously prepared 5 μm thick tissue sections were deparaffinized, dehydrated, and then treated with 0.3% H_2O_2 and incubated in citrate buffer for antigen retrieval. Sections were treated with rabbit polyclonal anti-TNF-α antibody (ab6671, Abcam, Cambridge, UK), and rabbit polyclonal anti- BMP-4 antibody (ab124715, Abcam, Cambridge, UK). After washing, incubation, and visualization with 3,3′-Diaminobenzidine (ab64238, Abcam, Cambridge, UK), the samples were embedded with entellan (Sigma-Aldrich, St. Louis, MO, USA) and examined under the light microscope in conjunction with a video camera.

Quantification of immunohistochemical staining was analyzed on previously recorded photomicrographs using the computer program cellSense v3.2. Photomicrographs taken at 200× magnification were subjected to intensity separation, its conversion to black and white, and background signal subtraction. The regions of interest were determined and placed on the obtained image display, and the final result was shown as the mean value of the color intensity—mean gray value. Histological and immunohistochemical examination were blindly performed by one investigator (O.C.P.).

4.5. Radiological Assessment

Cone beam computed tomography (CBCT) scans were performed with the three-dimensional (3D) Promax (Planmeca OY, Helsinki, Finland). The scan was performed with a resolution of 0.3 mm (scan time: 8.5 s, exposure time: 4 s, 120 kV, 5 mA). Radiographic assessment was performed at two time points. The first time point was before tooth extraction, and the second was at follow-up 4 months after extraction and augmentation. Identical configurations were used in both time periods. Radiological assessment was performed by measuring the width of the alveolar ridge (buccolingual dimension) at two time points. The width of the alveolar ridge was defined as the distance between the most prominent points buccally and orally (Figure 7). All measurements were performed by a single investigator (M.O.).

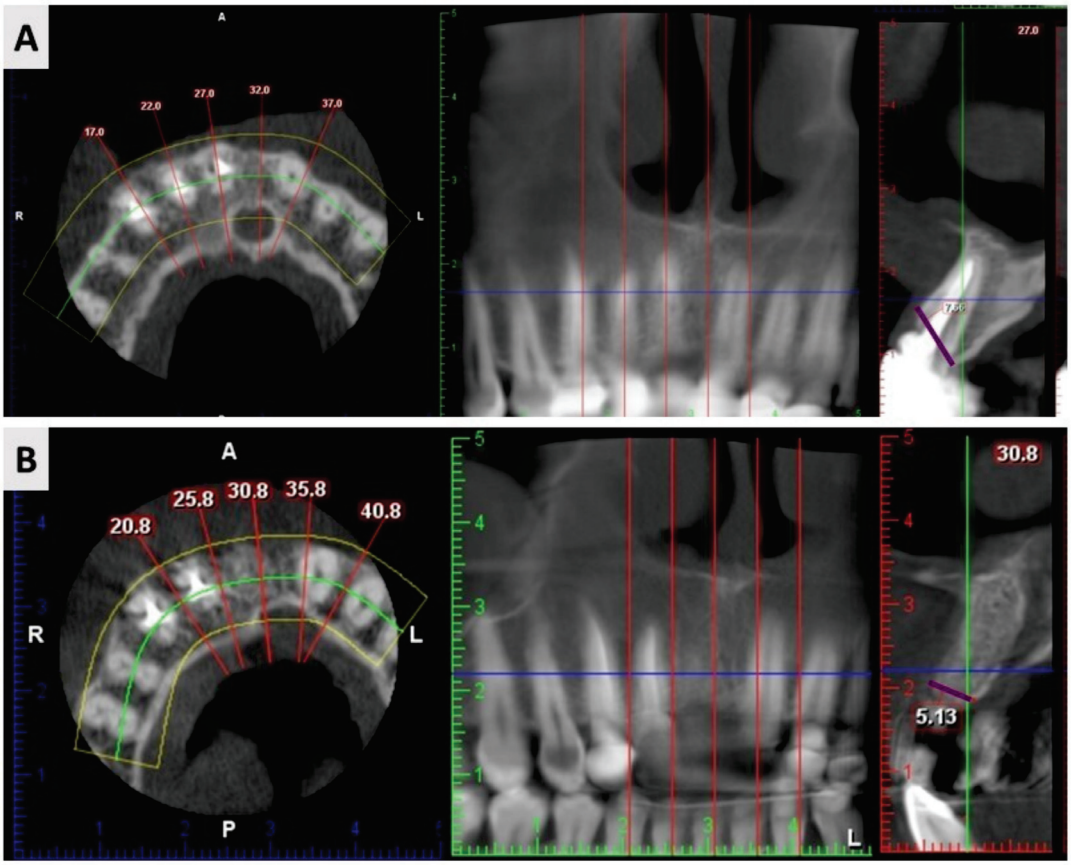

Figure 7. CBCT assessment protocol. The buccolingual dimension was measured between the most prominent points buccally and orally (purple marked line) at two time points—before extraction (**A**) and four months after (**B**).

4.6. Statistical Analysis

All data were transferred to a Microsoft Excel spreadsheet. Statistical analysis was performed using IBM SPSS Statistics (25.0, SPSS Inc., Chicago, IL, USA). Kolmogorov–Smirnov test was used to test the normality of the distribution. The data were normally

10 cm long incision was applied at the medial side of the distal femur epiphysis 1 cm proximal of the knee joint capsule longitudinally and parallel to the bone axis. The cortical bone was reached through incision of the local muscles and by dissection of the periosteum.

Two 5 × 6 mm cylindrical holes were drilled in the femoral epiphysis by using a water-cooled trephine. A minimal distance of 20 mm was kept in between the drilled holes to reduce the risk of fracture and to ensure proper healing and harvesting of the bone specimens at the end of the study.

The defects were filled with either BioM1 or BioM2. Prior to insertion of the biomaterials, the holes were dried using sterile cotton balls. When relative dryness was reached, the gel-like biomaterials were quickly injected in 2 mm thick layers and instantly photopolymerized for 40 s each using a calibrated dental light curing unit (Bluephase, 830 mW/cm^2, Ivoclar–Vivadent, Ellwangen, Germany). Polymerzation is shown in Figure 7a. After the bone defects were completely filled, the surface of each polymerized biomaterial was whipped once with a 70% ethanolic solution (Figure 7b). The position of the filled defects sites was marked by insertion of a 4 mm long titanium pin (Geistlich Biomaterials, Baden-Baden, Germany). The position of the pin in relation to the defect sites was transferred to a transparent plastic foil which was used for relocation after euthanasia. Subsequently, the periosteum was closed and the muscle fascia, subcutaneous tissue and skin were sutured with an absorbable thread.

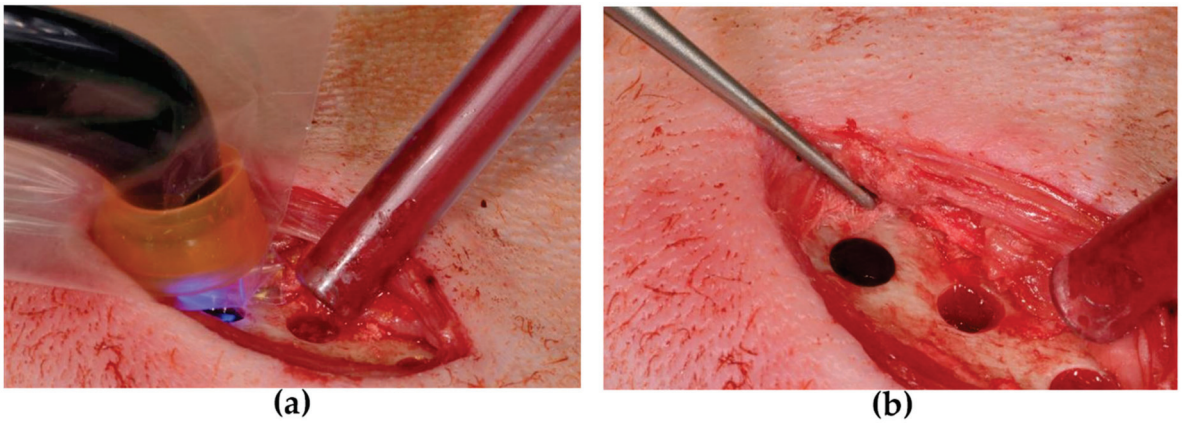

Figure 7. Biomaterial application: (**a**) light-polymerization; (**b**) solid biomaterial in the femur.

Afterwards, a second approximately 5 cm long incision was applied at the medial side of the proximal tibial epiphysis 1 cm distal of the knee joint capsule longitudinally and parallel to the bone axis. The cortical bone was exposed as described above and another defect of identical dimension was prepared and obturated by the identical biomaterial as already implanted into the femur.

After marking the location of the implant sites using a titanium pin and plastic foil, a suture was applied. Finally, both surgical sites were dressed with an aluminum based wound spray and medio-lateral as well as dorso-plantar X-ray images were taken as controls and for documentation of the healing progress. The location and total number of filled defect sites are summarized in Table 1. Antimicrobial prophylaxis and post-surgical pain control were applied. Animals were euthanized after 12 months of biomaterial implantation using a standardized protocol.